

## CHAPTER 300

### Numerical modeling of sediment transport for various mode

Masanobu ONO<sup>1)</sup>, Ichiro DEGUCHI<sup>2)</sup> and Toru SAWARAGI<sup>3)</sup>

#### **Abstract**

There are various mode of sediment transport on sandy beach. They are bed load, suspended load and sheet flow. Until now, various kinds of numerical model for analyzing these sediment transport have been developed based on the assumption of each mode of sediment transport. Consequently, it is difficult to apply them to different mode of sedimentation.

In this study, we propose a relatively simple numerical model for simulating sediment motion of various mode based on the semi-multi-phase flow model. The applicability of the model to sheet flow transport and suspended load transport is examined by using existing experimental data.

The results show that for the suspended sediment, it is necessary to take into the effect of the vortex to lift up sediment to high position. To construct numerical model for simulating sediment transport phenomena of the various mode, we have to introduce generation, development and disappearance process of bed ripple in this model.

#### **Introduction**

Mode of sediment transport continually changes from bed load, suspended load to sheet flow according to the increase in magnitude of agitation force. Until now, various kinds of numerical model for analyzing these sediment transport have been developed. An advection-diffusion equation has been widely used to analyze suspended sediment concentration. Suspended load is expressed as the product of concentration and migration speed of suspended sediment that is assumed to be equivalent to water particle velocity when the concentration is not so high. Concentration of bed load and sheet flow has also been analyzed by solving the advection-diffusion equation and the migration speed is estimated by solving a momentum equation of multi-phase flow. When we analyze sediment motion by these model, we have to know the mode of sediment transport before we determine what kind of model we should use.

---

1) Research Assoc., and 2) Assoc. Prof., Dept. of Civil Engineering, Osaka University, Yamada-oka, Suita, Osaka, 565, Japan

3) Prof., Dept. of Civil Engineering, Osaka sangyo University, Japan

In this study, we propose a relatively simple numerical model for simulating sediment motion of various mode based on the semi-multi-phase flow model. The applicability of the model to sheet flow transport and suspended load transport is examined by using existing experimental data. The effect of vortex shedding from the rippled bed on the Schmidt number is also investigated numerically.

## **Numerical simulation method for analyzing sediment transport**

### **(1)Basic equations**

Numerical model consists of a horizontal momentum equation of one-phase flow and equations of mass conservation of two-phase flow. There are generally six equations, that is, conservation of mass and conservation of horizontal and vertical momentum flux for sediment phase and fluid phase.

The continuity equations for sediment and water phase are shown by Eq.(1) and Eq.(2).

$$\frac{\partial \rho_s c}{\partial t} + \frac{\partial \rho_s c u_s}{\partial x} + \frac{\partial \rho_s c w_s}{\partial z} = 0 \quad (1)$$

$$\frac{\partial \rho_f (1-c)}{\partial t} + \frac{\partial \rho_f (1-c) u_f}{\partial x} + \frac{\partial \rho_f (1-c) w_f}{\partial z} = 0 \quad (2)$$

where  $c$  is volumetric concentration of sediment,  $\rho_s$  and  $\rho_f$  are the density of sediment and water,  $u_s$  and  $u_f$  are horizontal velocity of sand and water particle,  $w_s$  and  $w_f$  are vertical velocity of sand and water particle.

The momentum equations for sediment and water phase are shown by Eqs.(3),(4) and Eqs.(5),(6).

$$\frac{\partial \rho_s c u_s}{\partial t} + \frac{\partial \rho_s c u_s^2}{\partial x} + \frac{\partial \rho_s c u_s w_s}{\partial z} = -c \frac{\partial p}{\partial x} + \frac{\partial r_{xx}}{\partial x} + \frac{\partial r_{zx}}{\partial z} + f_x \quad (3)$$

$$\frac{\partial \rho_s c w_s}{\partial t} + \frac{\partial \rho_s c u_s w_s}{\partial x} + \frac{\partial \rho_s c w_s^2}{\partial z} = -c \frac{\partial p}{\partial z} + \frac{\partial r_{xz}}{\partial x} + \frac{\partial r_{zz}}{\partial z} - \rho_s c g + f_z \quad (4)$$

$$\frac{\partial \rho_f (1-c) u_f}{\partial t} + \frac{\partial \rho_f (1-c) u_f^2}{\partial x} + \frac{\partial \rho_f (1-c) u_f w_f}{\partial z} = -(1-c) \frac{\partial p}{\partial x} - f_x \quad (5)$$

$$\frac{\partial \rho_f (1-c) w_f}{\partial t} + \frac{\partial \rho_f (1-c) u_f w_f}{\partial x} + \frac{\partial \rho_f (1-c) w_f^2}{\partial z} = -(1-c) \frac{\partial p}{\partial z} - \rho_f (1-c) g - f_z \quad (6)$$

where  $p$  is pressure,  $f_i(i=x,z)$  is the  $i$ -th component of interaction force per unit volume between sediment and water,  $r_{ij}$  is inter granular stress tensor.

There are six unknowns,  $p$ ,  $u_f$ ,  $w_f$ ,  $u_s$ ,  $w_s$ , and  $c$ . However, it is very difficult to get stable numerical results of these equations due to very strong non-linear interaction of each equations, Therefore in our model we use the horizontal momentum equations and mass conservation equations and apply empirical relation for determining vertical velocity of sediment phase.

### **(2)Numerical simulation method**

To construct numerical model we made some assumptions and simplification. One is that the horizontal velocity of moving sand is the same as the horizontal fluid velocity. This implies that we apply single layer model for the sediment larded water and Eqs.(3) and (5) become Eq.(7) as shown below:

$$\begin{aligned} \frac{\partial}{\partial t} \left\{ \rho u - (\rho_s - \rho_f) k_x \frac{\partial c}{\partial x} \right\} + \frac{\partial}{\partial x} \left\{ \rho u^2 - 2u(\rho_s - \rho_f) k_x \frac{\partial c}{\partial x} - (\mu_e + \rho \Omega_x) \frac{\partial u}{\partial x} \right\} \\ + \frac{\partial}{\partial z} \left[ \left\{ (1-c) \rho w_f + c \rho_s w_s \right\} u - (\mu_e + \rho \Omega_z) \frac{\partial u}{\partial z} \right. \\ \left. - u(\rho_s - \rho_f) k_z \frac{\partial c}{\partial z} - (\rho_s w_s - \rho_f w_f) k_x \frac{\partial c}{\partial x} \right] = - \frac{\partial p}{\partial x} \quad (7) \end{aligned}$$

where  $u$  ( $=u_s=u_f$ ) is the horizontal velocity of sand and fluid particle and  $\mu_e$  is apparent viscosity of sediment laden water (Savage-McKeown, 1983).

Sediment concentration  $C$  is calculated from the continuity equation for the sediment phase Eq. (1) by transforming it into an advection-diffusion equation with diffusion coefficient  $k_i$  as follows:

$$\frac{\partial c}{\partial t} + \frac{\partial cu}{\partial x} + \frac{\partial cw_s}{\partial z} = \frac{\partial}{\partial x} \left( k_x \frac{\partial c}{\partial x} \right) + \frac{\partial}{\partial z} \left( k_z \frac{\partial c}{\partial z} \right) \quad (8)$$

Eq.(9) is derived from Eq.(2) by performing the same transform.

$$- \frac{\partial c}{\partial t} + \frac{\partial(1-c)u}{\partial x} + \frac{\partial(1-c)w_f}{\partial z} = - \frac{\partial}{\partial x} \left( k_x \frac{\partial c}{\partial x} \right) - \frac{\partial}{\partial z} \left( k_z \frac{\partial c}{\partial z} \right) \quad (9)$$

The diffusion coefficient is assumed to be proportional to the kinematic eddy viscosity  $\Omega_i$  by using Schmidt number  $Sm$  as follow.

$$k_x = \Omega_x / Sm \quad k_z = \Omega_z / Sm \quad (10)$$

$$\mu_e = 1.2\lambda^2 \mu_0 \quad \lambda = 1 / \left\{ (c_{\max} / c)^{1/3} - 1 \right\} \quad (11)$$

where  $\mu_0$  is water viscosity,  $\lambda$  is the Linear concentration,  $c_{\max}(=0.65)$  is the maximum possible static concentration of uniform spheres. We used the expression for kinematic eddy viscosity proposed by Nadaoka et al.(1990).

$$\Omega_x = l_{(z)}^2 \left| \frac{\partial u}{\partial x} \right| \quad \Omega_z = l_{(z)}^2 \left| \frac{\partial u}{\partial z} \right| \quad l_{(z)} = \kappa \int_{-\infty}^z (c_{\max} - c) / c_{\max} dz \quad (12)$$

where  $l(z)$  is mixing length and  $\kappa$  is Karman constant.

To evaluate the vertical velocity of sediment phase, an empirical expression to relate settling velocity of sand particle and concentration is used.

$$w_s = -w_{s0} \left( 1 - c / c_{\max} \right)^{2.3} \quad (13)$$

where  $w_{s0}$  is the settling velocity of sand particle in clear water.

Vertical velocity of water particle is calculated by the continuity equation for two phase flow. Eq.(14) is derived from Eqs.(8) and (9).

$$\frac{\partial u}{\partial x} + \frac{\partial}{\partial z} \left\{ cw_s + (1-c)w_f \right\} = 0 \quad (14)$$

Equations (7),(8),(13) and (14) were simultaneously solved by transforming them into finite difference equations. In this model, horizontal phenomena is assumed to be homogeneous in the direction of wave propagation.

**(3)Initial and boundary conditions**

Z axis is taken upward from the initial sand surface as shown in Fig.1. The up-ward boundary conditions are given by Eqs.(15) and (16) at the boundary layer whose thickness is given by Eq.(17).

$$c w_s + k_z \frac{\partial c}{\partial z} = 0 \quad (15) \qquad u = U_0 \sin(\sigma t) \quad (16)$$

$$\max(D_z) = 4\kappa \max(u^*)/\sigma \qquad u^* = |v_z| \frac{\partial u}{\partial z} \quad (17)$$

The pressure gradient in Eq.(7) is given by the pressure gradient outside the boundary layer using the expression of Eq.(16).

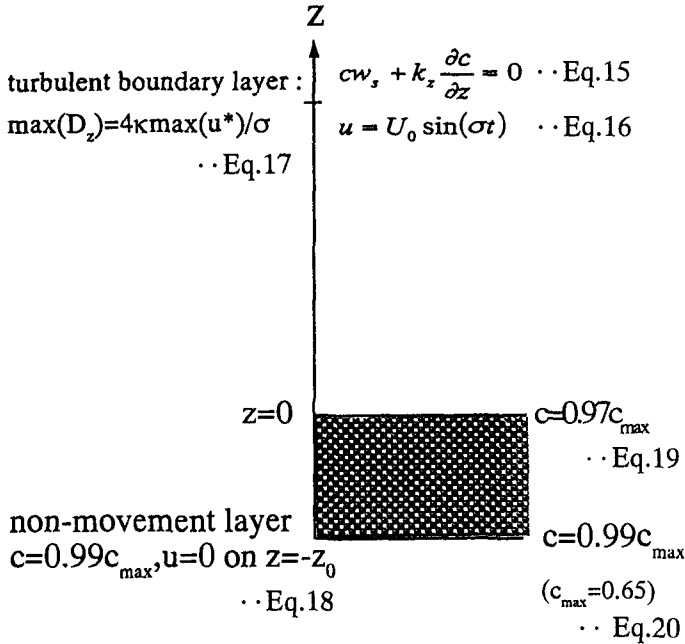


Fig. 1 Coordinate system

Two boundary conditions at the bottom are applied. One is the velocity of sediment laden water is 0 and the other is sediment concentration is  $0.99c_{max}$ . These are given at assumed initial thickness of sand layer  $z=-z_0$ . To prevent dispersion of vertical gradient of apparent viscosity near sand surface, we distribute sediment concentration in sand layer from  $0.97c_{max}$  to  $0.99c_{max}$  between  $z=-z_0$  and  $z=0$  linearly. Calculations are started from the still water and there is no suspended sediment concentration in the region of  $z$  is greater than 0.

The thickness of moving sand layer is determined by using Bagnold's condition as shown by Eq.(21).

$$\mu_e \frac{\partial u}{\partial z} \geq \int_z^{+\infty} (\rho_s - \rho_f) g c \tan \phi dz \quad (21)$$

The friction angle  $\phi$  in Eq. (21) also depends on sediment concentration. When the linear concentration is smaller than 1, there is no resisting force against shear. We assume that the value usually used for  $\phi$  is applicable when the linear concentration is larger than 14. It is said that fluid act as a Newtonian fluid when the linear concentration is smaller than 14. We change the value of  $\phi$  continuously in this region as shown by Eq. (23).

$$\mu_e \frac{\partial u}{\partial z} \geq \int_z^{+\infty} (\rho_s - \rho_f) g c \tan(\alpha\phi) dz \quad (22)$$

$$\alpha = \lambda / \lambda_{14} \quad \lambda \leq 14 (c \leq 0.53)$$

$$\alpha = 1 \quad 14 \leq \lambda (0.53 \leq c) \quad (23)$$

### Applicability of the model under sheet flow and suspended sediment conditions

We carried out a series of calculation under various conditions. Here, the calculated results are compared with experimental results under sheet flow condition reported by Horikawa et al.(1982) and experimental results under pure suspension condition given by Nakato et. al.(1977) to examine the applicability of the numerical method. There was not any bottom configuration in the former experiments and there were ripples on the bottom in the latter experiments. Both of the experiments were carried out in oscillatory flow tunnels.

Figures 2 and 3 show the comparisons of calculated and measured horizontal velocity, concentration profile. Fig. 4 is the thickness of moving sand layer under the same experiment (Horikawa et. al.(1982)). In these calculation we assumed that the value of Schmidt number was 10. Measured velocity, concentration and thickness of moving layer are roughly reproduced by the numerical simulation.

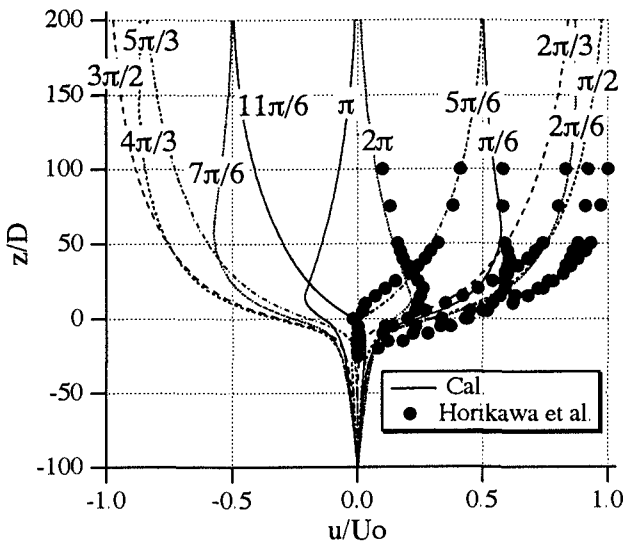


Fig. 2 Comparison between Horikawa's experimental results and calculated results under sheet flow condition (Horizontal velocity profile, Schmidt number :Sm=10)

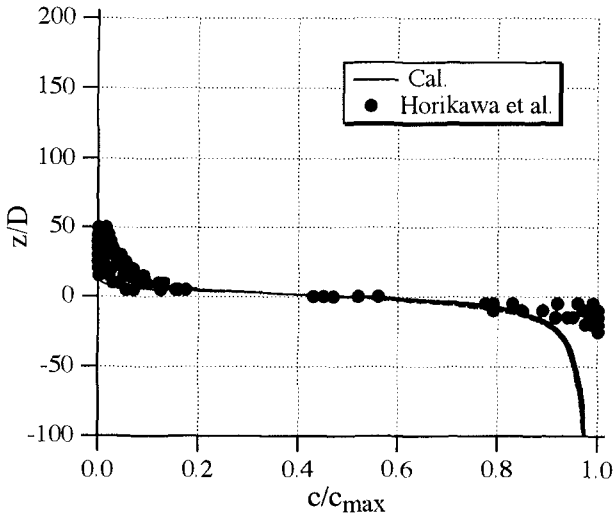


Fig. 3 Comparison between Horikawa's experimental results and calculated results under sheet flow condition (Sediment concentration profile,  $Sm=10$ )

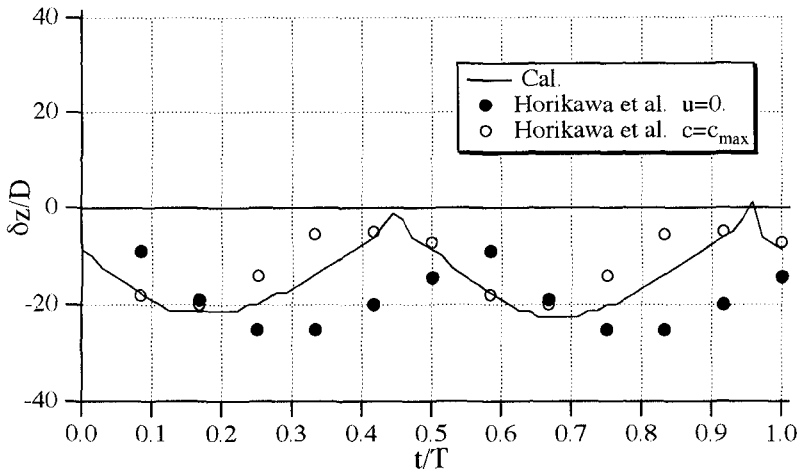


Fig. 4 Comparison between Horikawa's experimental results and calculated results under sheet flow condition (Thickness of moving layer,  $Sm=10$ )

We calculate the vertical distribution of purely suspended sediment concentration given by Nakato and others by using the same Schmidt number, that is  $Sm=10$ . In Figs.5 and 6, some examples of calculated results (shown by solid line) are compared with the measured results. As can be seen from this figure, we could not reproduce the measured distribution by the calculation.

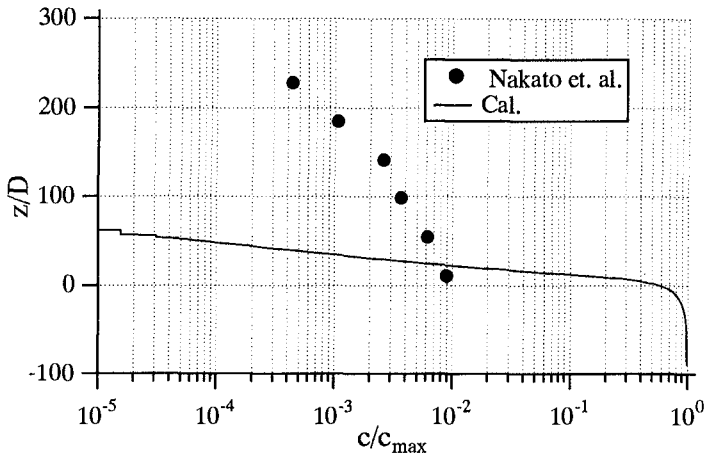


Fig. 5 Comparison between Nakato's experimental results and calculated results under suspended sediment condition (sediment concentration profile ,Case1,  $S_m=10$ )

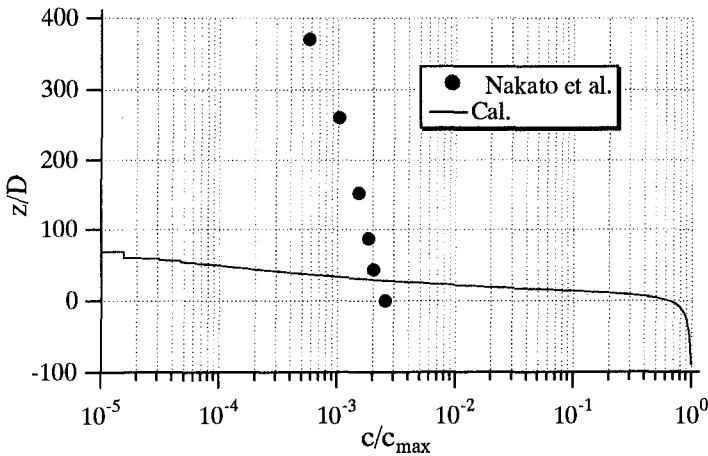


Fig. 6 Comparison between Nakato's experimental results and calculated results under suspended sediment condition (sediment concentration profile ,Case2,  $S_m=10$ )

The reason for this discrepancy was simply because the kinematic eddy viscosity did not diffuse from the horizontal bottom and diffusion coefficient outside the boundary layer become almost 0. To improve our numerical model, we changed the value of Schmidt number from bed load layer to suspended load layer. In the bed load layer, the same value of Schmidt number as the sheet flow is used and for the suspended load layer, the value is reduced to be 0.5 to increase diffusion coefficient. We defined the bed load layer where the concentration is lower than the reference concentration given by Sawaragi et al.(1985).

The calculated results are shown by broken lines in Figs. 7 and 8. The degree of agreement between measured and calculated concentration is improved. This

implies that the flow field, especially structure of turbulence in the sheet flow region and suspended load layer is perfectly different from each other and systematic vortices generated by the ripples play an important role in the purely suspended load layer.

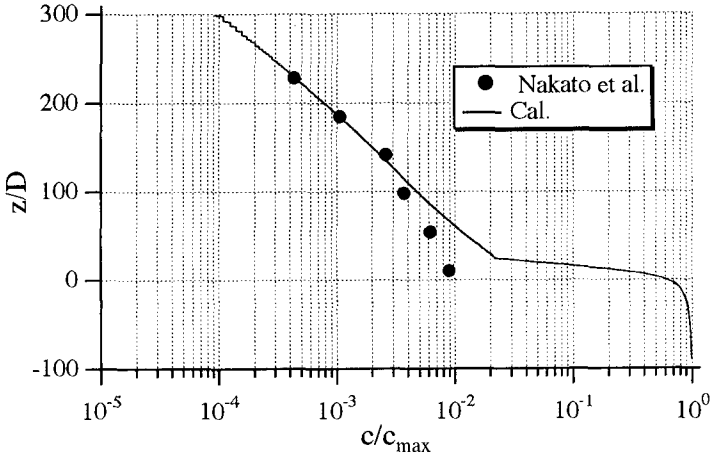


Fig. 7 Comparison between Nakato's experimental results and calculated results under suspended sediment condition (Case1, Suspended load layer : $S_m=0.5$ , Bed load layer : $S_m=10$ )

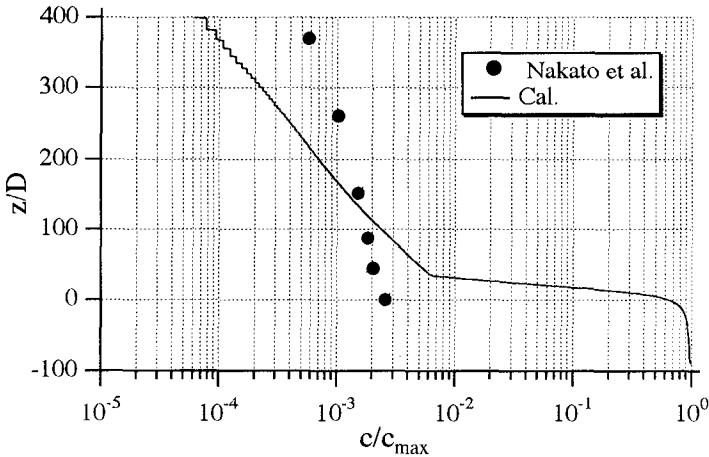


Fig. 8 Comparison between Nakato's experimental results and calculated results under suspended sediment condition (Case2, Suspended load layer : $S_m=0.5$ , Bed load layer : $S_m=10$ )

**Diffusion coefficient of suspended sediment on the ripple bed**

To investigate flow field and the effect of the systematic generation of vortex on rippled bottom, we calculated vortex flow field on ripple bed by modified vortex

filament method originally proposed by Longuet-Higgins(1981). We used circular vortex instead of vortex filament to avoid velocity from going infinity. Eqs.(24) and (25) are the complex velocity potential of circular vortex used in the analysis.

$$|W - W_n| > Gr \Rightarrow \frac{\Gamma_n}{2\pi i} \ln(W - W_n) \quad (24)$$

$$|W - W_n| < Gr \Rightarrow \frac{\Gamma_n}{2\pi i} \frac{1}{Gr} (W - W_n) \quad (25)$$

where  $W$  is the arbitrary point in the interior of the unit circle on the complex number plane,  $W_n$  is the position of circular vortex,  $\Gamma_n$  is the circulation of circular vortex,  $Gr$  is the radius of circular vortex that will be determined from the comparison of measured and calculated turbulence intensity of horizontal velocity on the ripples. When the distance between  $W$  and  $W_n$  is longer than  $Gr$ , the complex velocity potential becomes the same equation of vortex filament. But when  $W_n$  approaches to  $W$ , the complex velocity potential converges to 0.

Decay of circulation of separated vortex is reproduced by decreasing circulation of each circular vortex by assuming the following time variation with the damping coefficient  $\alpha_G$  :

$$\Gamma_n = \Gamma_{on} \exp(-\alpha_G t_{0n} / T) \quad (26)$$

where  $\Gamma_{on}$  is the initial circulation of n-th circular vortex,  $t_{0n}$  is the elapsed time since n-th circular vortex has been released. The damping coefficient will also be determined from the measured time variation of vortex circulation.

Solid lines in Fig.9 show the calculated time variation of circulation under various values of damping coefficient. In the figure, measured time variation of circulation of separated vortex (Horikawa et al.,1992) is also shown. Fig. 11 shows the comparison of measured turbulent intensity of horizontal velocity on the ripples (Sawamoto et al.,1981) and calculated result by giving various values of radius for the circular vortex. The vertical axis  $z$  is the distance upward from the ripple crest.

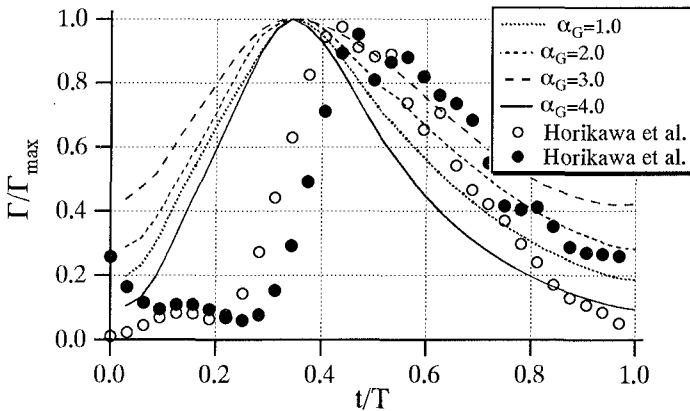


Fig. 9 Time variation of circulation of separated vortex

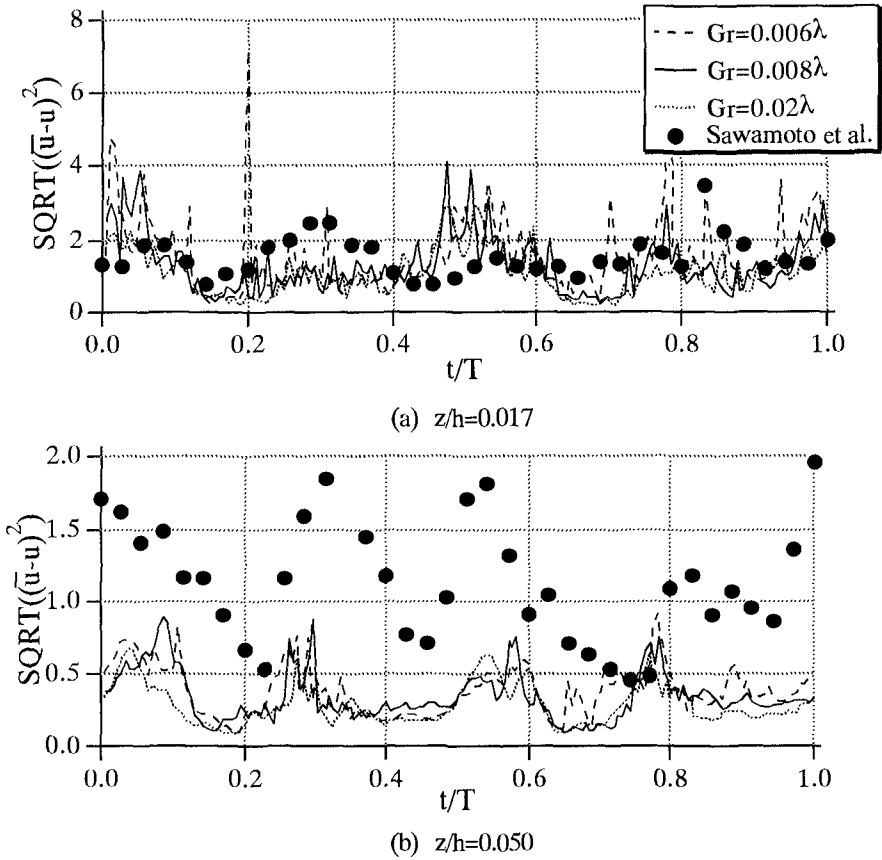


Fig. 10 Vertical distribution of turbulent intensity of horizontal velocity

By comparing calculated and measured result of time decay of circulation and turbulent intensity, circular vortex radius is determined to be 0.8% of ripple length and vortex circulation damping coefficient to be 4.

**Calculation of diffusion coefficient of suspended sediment**

The motions of suspended sediment are calculated in the flow field obtained on the ripples by an above-mentioned procedure. The governing equations of sediment motion are horizontal and vertical equations of motion as shown in non-dimensional forms by Eqs.(27) and (28) and are solved by using the forth-order Runge-Kutta method.

$$\frac{\partial u_s^*}{\partial t^*} = \frac{3}{4} \frac{1}{\rho_s^* + C_M} C_D K_C |u_f^* - u_s^*| (u_f^* - u_s^*) + \frac{\partial u_f^*}{\partial t^*} \tag{27}$$

$$\frac{\partial w_s^*}{\partial t^*} = \frac{3}{4} \frac{1}{\rho_s^* + C_M} C_D K_C |w_f^* - w_s^*| (w_f^* - w_s^*) + \frac{\partial w_f^*}{\partial t^*} - \frac{\rho_s^* - 1}{\rho_s^* + C_M} g^* \quad (28)$$

$$t^* = t\sigma, (u_s^*, w_s^*) = (u_s, w_s) / w_{s0}, (u_f^*, w_f^*) = (u_f, w_f) / w_{s0},$$

$$\rho_s^* = \rho_s / \rho_f, g^* = g / (w_{s0}\sigma) \quad (29)$$

where  $R_e = w_{s0}D/\nu$ ,  $K_C = w_{s0}/D\sigma$ ,  $C_M = 1/2$ ,  $g$  is the gravity acceleration,  $\sigma$  is the angular frequency and  $C_D$  is the drag coefficient. The variables with ' in Eqs.(27) and (28) are dimensionless normalized by relation shown by Eq.(29).

To evaluate drag coefficient  $C_D$  we adopted the following expression of Molerus and Werther(1968):

$$C_D = \frac{24}{R_e} \left( \frac{1}{|w_f^* - w_s^*|} + \frac{0.152}{\sqrt{|w_f^* - w_s^*|}} + 0.0151R_e \right) \quad (31)$$

Initial positions of sand particles are distributed on the ripples as shown Fig.11. and they are released four cycles after calculation of the flow field where the flow becomes steady and stable. The motion of sand particles is calculated for seven cycles.

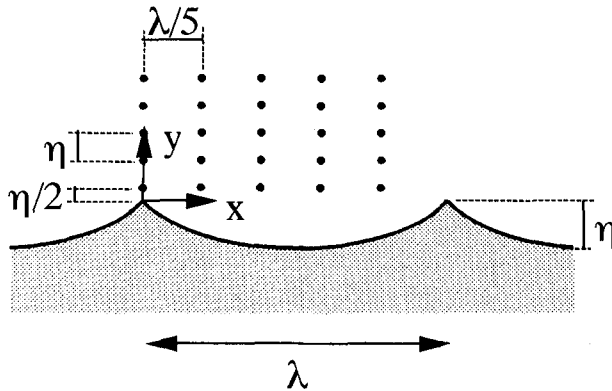


Fig. 11 Coordinate system and initial arrangement of sand particles

Diffusion coefficient of suspended sediment is evaluated by the calculated displacement of sand particles by Eq.(32).

$$k_z(t) = \frac{1}{2} \frac{d \left\{ \sum_{i=1}^{25} l_i(t)^2 / 25 \right\}}{dt} \quad (32)$$

where  $l(i)$  is relative position vector of sand particles evaluated by Eq.(33).

$$l_i(t) = s_i(t) - S(t) \quad (33)$$

where  $s_i(t)$  is the position of  $i$ -th sand particle,  $S(t)$  is the average position of all sand particles.

Fig.12 shows the comparison of the calculated and measured diffusion coefficient of suspended sediment. Calculated results show good agreement with the measured diffusion coefficient. This means that systematic vortex shedding from the ripple bed plays very important role in sediment suspension. It is not necessary for the sediment movement under the sheet flow condition that takes place on a flat bed to exist such kind of systematic vortex. For the suspended sediment, it is necessary to take into the effect of the vortex to lift up sediment to high position.

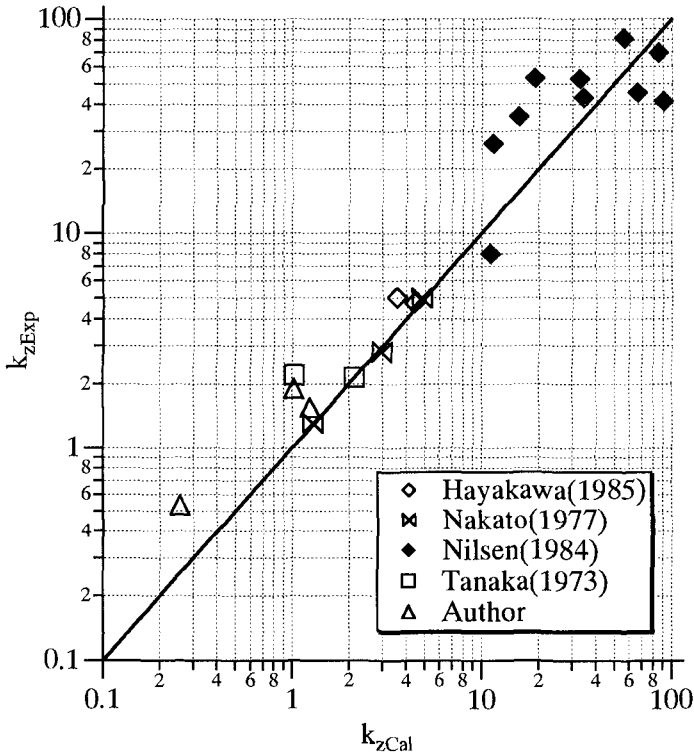


Fig. 12 Comparison of measured and calculated diffusion coefficient

## Conclusions

We propose a relatively simple numerical modeling of sediment transport for various mode based on the semi-multi-phase flow model and examine the applicability of the model by using existing experimental results of sheet flow and suspended sediment. Although calculated results roughly reproduce the experimental results under sheet flow condition, we could not predict vertical distribution of the concentration of the suspended sediment.

To investigate this reason, we examine the suspended sand particle motion in vortex flow on the ripples. The diffusion coefficient that is evaluated by analyzing sand particle motions on ripples is coincide with the experimental results. This result implies that systematic vortices generated by the ripples lift up suspended sediment to

high position. Therefore to construct numerical model for various mode of sediment transport, we have to introduce generation, development and disappearance process of bed ripple in the model.

### Reference

- Savage S. B. and S. McKeown : Shear stresses developed during rapid shear of concentrated suspensions of large spherical particles between concentric cylinders. *J. Fluid Mech.*, Vol. 127, pp.453-472,1983.
- Nadaoka, K. and H. Yagi: Single-phase fluid modeling of sheet flow toward the development of "Numerical mobile bed", Proc. 22nd Coastal Eng. Conf., ASCE, pp.2346-2359, 1990.
- Horikawa, K., A. Watanabe and S. Katori: Sediment transport under sheet flow condition, Proc. 18th Coastal Eng. Conf., ASCE, pp.1335-1352, 1982.
- Nakato T., F. A. Locher, J. R. Glover and J. F. Kennedy : Wave entrainment of sediment from rippled beds, *A.S.C.E., WW1*, Vol. 103, pp.83-99, 1977.
- Sawaragi T., J. S. Lee, and I. Deguchi: A new model for a prediction of beach deformation around a rivermouth, Proc. Int'l Sympo. on Ocean Space Utilization '85, pp.229-236, 1985.
- Longuet Higgins, M. S.: Oscillating flow over steep sand ripples, *J. Fluid Mech.*, Vol. 107, pp.1-35, 1981.
- Horikawa, K. and S. Mizutani: Oscillatory flow behavior in the vicinity of ripple models, Proc. 23rd Coastal Eng. Conf., ASCE, pp.2122-2135, 1992.
- Sawamoto M., T. Yamashita, and T. Kitamura: Distributions of turbulence intensity and suspended sediment concentration over rippled beds, Proc. 29th Japanese Conf. Coastal Eng., pp.232-236, 1981. (in Japanese)
- Molerus, O. and J. Werther: Berechnung der Sinkbewegung kugeligter teilchen in einem vertikal pulsierenden stromungsfeld, *Chemie-Ingenieur-Technik*, Vol. 40, pp.522-524, 1968.
- Hayakawa, N., G. Tsujimoto and H. Hashimoto, Velocity distribution and suspended sediment concentration over large scale ripple, *Coastal Eng. in Japan*, Vol. 26, pp.91-100,1983.
- Nielsen, P.: Field measurements of time averaged suspended sediment concentration under waves, *Coastal Eng.*, Vol. 8, No. 1, pp.51-72, 1984.
- Tanaka, N., H. Ozawa and A. Ogasawara, Experiments on sand movement by waves and currents, Rept. Port and Harbour Res. Inst., Vol. 12, No.4, pp.2-22,1973,(in Japanese).